Parity-odd Neutrino Torque Detection

Hao-Ran Yu,[1,2,3,*] Ue-Li Pen,[2,1,4,5,6,†] and Xin Wang[2,‡]

[1] *Tsung-Dao Lee Institute, Shanghai Jiao Tong University, Shanghai, 200240, China*
[2] *Canadian Institute for Theoretical Astrophysics, University of Toronto, M5S 3H8, Ontario, Canada*
[3] *Department of Astronomy, Shanghai Jiao Tong University, Shanghai, 200240, China*
[4] *Dunlap Institute for Astronomy and Astrophysics, University of Toronto, Toronto, ON M5S 3H4, Canada*
[5] *Canadian Institute for Advanced Research, CIFAR Program in Gravitation and Cosmology, Toronto, ON M5G 1Z8, Canada*
[6] *Perimeter Institute for Theoretical Physics, Waterloo, ON N2L 2Y5, Canada*

(Dated: October 20, 2018)

Cosmological observations are promising ways for discovering the neutrino mass properties. The upper bound on their sum of mass is given by the cosmic microwave background and large scale structures. These measurements are all parity-even. Here we show that, the presence of neutrino mass provides a unique contribution to the directions of the angular momentum of galaxies, which is the first parity-odd neutrino effect on large scale structures. This parity-odd observable is free of the contamination of the linear perturbation theory, and can be cleanly separated from other non-gravitational effects. A complete 21-cm neutral Hydrogen halo survey deep to redshift 1 can give a 5σ confidence level of detecting the neutrino torque effect if the sum of neutrino masses is 0.05 eV.

Introduction.— Neutrino mass is a long-standing physics problem. The flavour oscillation experiments [1] discovered the mass splittings of neutrinos and placed a lower bound of the sum of their mass $M_\nu \equiv \sum_{i=1}^{3} m_{\nu_i} \gtrsim 0.05$ eV [2]. The existence of neutrino mass has profound impacts on cosmic evolution. In the early Universe relativistic neutrinos modulate the matter-to-radiation ratio, and based on which the cosmic microwave background observations provide an upper bound of $M_\nu \lesssim 0.23$ eV [3]. In the late Universe, neutrinos become non-relativistic, and contribute to the matter energy density Ω_m. Unlike the majority of matter, the cold dark matter (CDM) and baryons, neutrinos maintain a high velocity dispersion, known as "free streaming", which reduces their gravitational collapse on small scales. A number of large scale structure (LSS) surveys (such as Euclid [4], LSST [5], eBOSS [6], WFIRST[7], and DESI [8]) are aimed to improve this upper bound using neutrino effects on LSS, however we usually encounter difficulties in disentangling neutrino effects from other parameters, and in understanding halo bias and cosmic variance. Recently, new nonlinear neutrinos effects on LSS are proposed to give independent measurements on neutrino mass [9–11]. Here we present a novel neutrino torque effect which modulates the angular momenta (spin) of dark matter halos, which can be measured to constrain the neutrino mass.

Theory.— In the picture of LSS formation, gravitational instability lets initial density fluctuations form dark matter halos, in which galaxies are embedded. While in these highly nonlinear structures, uncertainties of halo bias, halo merging history and baryonic mechanisms obstruct us from clearly understanding the statistics like number counts and morphologies [12], the spins of galaxies/halos represent a clean structure formation history in the linear Universe, which are poorly appreciated.

The spin of a halo in Lagrangian space $\boldsymbol{j}_L \propto \int_{V_L} \boldsymbol{q} \times \boldsymbol{\nabla}\phi \mathrm{d}^3\boldsymbol{q}$ can be written in first order as $\boldsymbol{j}_I \propto \boldsymbol{\epsilon}\mathbf{I}\mathbf{T}$ [13], where ϕ is the gravitational potential, $\boldsymbol{q}$ is the Lagrangian coordinates relative to the center of mass of the protohalo in volume V_L, $\mathbf{I} = (I_{ij}) = (\int_{V_L} q_i q_j \mathrm{d}^3\boldsymbol{q})$ is the inertia tensor, $\mathbf{T} = (T_{ij}) = (\partial_i\partial_j\phi)$ is the tidal shear tensor, and $\boldsymbol{\epsilon} = (\epsilon_{ijk})$ is the Levi-Civita symbol. This picture shows that the initial spin of the protohalo is generated by the misalignment between the protogalactic inertia tensor and local gravitational shear tensor, and grows at first order in the early Universe [13]. Actually, as halos collapse, nonlinear gravity field is hard to torque small objects, and we expect the spin directions are contributed mostly in the linear regime. These can be straightforwardly tested in numerical simulations. The halo merging and baryonic feedback, usually been discussed in the halo/galaxy alignment studies, do not affect the angular momentum conservation, because connected/disconnected matter and baryonic matter in Lagrangian space are torqued by the same gravitational shear.

Neutrino density field traces CDM on large scales while smoothly distributed on small scales, because the free streaming of neutrinos makes them less susceptible to the total gravitational potential. This contributes to a predictable tidal tensor $\mathbf{T}_\nu(m_{\nu_i})$ depending on the their mass. Acting on the protogalactic inertia tensor $\mathbf{I}$ it generates an additional neutrino torque $\boldsymbol{j}_\nu^I \propto \boldsymbol{\epsilon}\mathbf{I}\mathbf{T}_\nu$. The inertia tensor $\mathbf{I}$ is also predictable by using the fact that protogalactic inertia $\mathbf{I}$ and the tidal field from CDM $\mathbf{T}_c$

* haoran@cita.utoronto.ca
† pen@cita.utoronto.ca
‡ xwang@cita.utoronto.ca

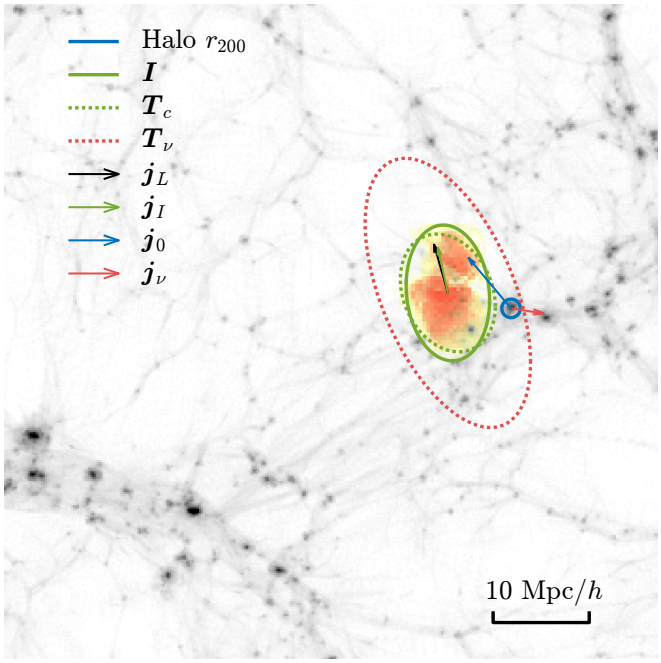

FIG. 1. Illustration of the initial spin direction $\boldsymbol{j}_L$ of a protohalo region, and its tidal torque theory prediction $\boldsymbol{j}_I$ calculated by the inertia tensor $\mathbf{I}$ and tidal shear tensor $\mathbf{T}_c$. The halo at present epoch is marked with the r_{200} circle with its spin direction $\boldsymbol{j}_0$, highly correlated with $\boldsymbol{j}_L$ and $\boldsymbol{j}_I$. We show that neutrino tidal torque $\boldsymbol{j}_\nu$ is generally uncorrelated with $\boldsymbol{j}_0$.

are highly correlated in Lagrangian space [14, 15], which can be understood that $\mathbf{I}$ is a collection of matter to be shell-crossed to form a halo, being parallel with $\mathbf{T}_c$.

To optimize the cross-correlation, we construct an equivalent inertia $\mathbf{I}_r$ from $\mathbf{T}_c$, in order that $\boldsymbol{\epsilon}\,\mathbf{I}_r\mathbf{T}_\nu$ is maximumly correlated with the integrated neutrino torque

$$\boldsymbol{j}^I_{\nu 0} = \int a(\tau)D(\tau)\boldsymbol{\epsilon}\mathbf{I}(\tau)\mathbf{T}_\nu(\tau)\mathrm{d}\tau. \tag{1}$$

In the primary coordinate of $\mathbf{T}_c$, $\mathbf{T}_c$ can be eigen-decomposed as $\mathbf{T}_c = \sum_{i=1}^3 \mathbf{T}_c^{\lambda_i}$ and find α_i such that the reconstructed

$$\mathbf{I}_r = \sum_{i=1}^{3} \alpha_i \mathbf{T}_c^{\lambda_i} \tag{2}$$

optimizes the cross-correlation $\mu(\boldsymbol{j}^I_{\nu 0}, \boldsymbol{j}^{I_r})$, where

$$\boldsymbol{j}^{I_r}_\nu = \boldsymbol{\epsilon}\,\mathbf{I}_r\mathbf{T}_\nu \tag{3}$$

is the reconstructed neutrino spin direction.

Simulation.— These correlations and coefficients are tested across a set of high-resolution N-body simulations [16]. Given any halo produced by the simulation, all the belonging particles are mapped back to Lagrangian space. The status of this definite set of particles can be traced in a resimulation, for example, their spin $\boldsymbol{j}(z) = \sum \boldsymbol{x}(z) \times \boldsymbol{v}(z)$ relative to their center of mass. In Fig.1 we plot (note that all quantities are projected onto the plane of this letter) the LSS from a simulation at redshift $z = 0$, and mark one selected halo with its r_{200} radius (within which the mean halo density is 200 times the mean matter density of the universe) and its spin direction $\boldsymbol{j}(z = 0)$ (all the spin arrows are normalized to have 15 Mpc/h). We illustrate Lagrangian mapping of this halo with its protohalo's column density (the orange clouds), with its initial spin direction $\boldsymbol{j}_L$. We can see that the Lagrangian spin $\boldsymbol{j}_L$ and Eulerian spin $\boldsymbol{j}_0$ have similar directions. Indeed, by averaging over all the halos in the simulation, we find the expectation value of the cross-correlation coefficient $\langle \boldsymbol{j}(z) \cdot \boldsymbol{j}_L \rangle$ is smoothly decreasing from unity to 0.80. This shows that the halo spin direction is conserved from the initial state all the way to the final state of the Universe.

We next examine the tidal torque formulation. To the first order approximation, the protohalo's inertia tensor $\mathbf{I}$ is represented by an equivalent ellipsoid (projected as a solid ellipse in Fig.1) with its volume equals to V_L. Similarly, the initial tidal shear tensor from CDM, $\mathbf{T}_c$, is shown the dotted green ellipsoid with same volume. The initial tidal shear from neutrinos, $\mathbf{T}_\nu$ is shown by the dotted red ellipsoid (8 times the volume of V_L, for clearity). The initial spins given by the tidal torque theory are the interplays between $\mathbf{I}$ and $\mathbf{T}_{c/\nu}$, shown in Fig.1) as $\boldsymbol{j}_I$ and $\boldsymbol{j}_\nu$. Obviously $\boldsymbol{j}_I$ has similar direction with $\boldsymbol{j}_L$ and $\boldsymbol{j}(z = 0)$, where as $\boldsymbol{j}_\nu$ gives an independent direction. From the initial condition to the end of the simulation, $\langle \boldsymbol{j}(z) \cdot \boldsymbol{j}_I \rangle$ decreases smoothly from 0.75 to 0.69. For neutrinos, the first-order tidal torque approximation gives a perfect (with cross-correlation 0.99) representation of the actual neutrino torque and it has generally less than 0.2 cross-correlation with CDM torques. This is expected in that $\mathbf{T}_c$ dominates locally (power spectrum index?) whereas $\mathbf{T}_\nu$ is contributed beyond the neutrino free-streaming scale (is this a 4-point function?). These two species, however, have a highly correlated contribution in structure formation. When we consider the forces that the two species exerted to the protohalo, $\boldsymbol{F}_{c/\nu} \propto \int_{V_L} \boldsymbol{\nabla}\phi_{c/\nu}\mathrm{d}^3\boldsymbol{q}$, the cross-correlation between two species is as high as 0.86 (power spectrum index?).

By Eq.(1) we estimate the magnitude of integrated neutrino torque $\langle |\boldsymbol{j}_{0\nu}|/|\boldsymbol{j}_0| \rangle \simeq 3 \times 10^{-4}$. In particular, the effect given by the smoother distribution for neutrinos relative to CDM accounts 0.03, while the neutrino fraction $f_\nu = 3.5 \times 10^{-3}$ (for $M_\nu = 0.05$ eV) and the backreaction from neutrinos to CDM $\sqrt{8}$ contribute the rest.

Measured from simulations, $(\alpha_1, \alpha_2, \alpha_3) = (-0.18, 0.18, 0.02)$ optimizes the cross-correlation $\left\langle \boldsymbol{j}^I_{\nu 0} \cdot \boldsymbol{j}^{I_r}_\nu \right\rangle = 0.19$. In this case we need 4×10^8 halos to have a 1σ detection (see Appendix A). If we improve the reconstruction of $\mathbf{I}_R$, the lower limit of required halos is 1.7×10^7.

Discussion.— Accuracy and mass dependency: we no-

tice that the cross-correlation coefficients between $\boldsymbol{j}_0$ and initial values $\boldsymbol{j}_L$ and $\boldsymbol{j}_T$ are prominently higher than what was measured in [14]. We investigate that numerical errors that may affect the results. P3M (particle-particle particle-mesh) algorithms result in higher cross-correlation between initial and final spins, compared to PM (particle-mesh), where additional tangential forces in PM violate the angular momentum conservation. Higher mass halos in a given simulation generally have slightly higher μ_L and μ_I, however the correlation is enhanced greatly as we use higher mass resolutions. All other cross-correlation measurements have only weak dependencies on the halo mass, even in a fixed simulation. With different box sizes, mass resolutions, force resolutions, and find that the results are consistent across these simulations. Especially, in the estimation of number of halo spins needed to detect the neutrino torque, the deciding number is the cross-correlation $\left\langle \boldsymbol{j}^I_{\nu 0} \cdot \boldsymbol{j}^{I_r}_{\nu} \right\rangle = 0.19$. This has a very weak dependence on halo mass and configuration of the simulation.

Reconstruction: to extract the neutrino torque from observable galaxy surveys, we need to reconstruct the initial conditions. There are many emerging successful reconstruction algorithms [17–19], mostly based on the E-mode clustering in Lagrangian space [20]. Least action algorithms.

Baryonic effects (+ etc.) in reconstruction and angular momentum conservation:

Observability: surveys like the Hubble Sphere Hydrogen Survey (HSHS) [21] can cover 1 billion galaxies.

Beyond standard models: it was also suggested that neutrino mass is generated by a gravitational θ-term condensation as the source of dark energy [22].

Cosmic variance:

Bias:

Conclusion.—

Acknowledgments.— We acknowledge funding from NSERC.

Appendix A: Errors in 3D

There are N halos with their unit spin vector randomly distributed on a 2D sphere, $|\boldsymbol{j}| = 1$ and $\langle \boldsymbol{j} \rangle = \boldsymbol{0}$. Adding an additional vector $a\hat{\boldsymbol{x}}$ ($a \ll 1$) to $\boldsymbol{j}$ and normalize we have $\boldsymbol{j}' = (\boldsymbol{j} + a\hat{\boldsymbol{x}})/|\boldsymbol{j} + a\hat{\boldsymbol{x}}|$, then we project $\boldsymbol{j}'$ onto $\hat{\boldsymbol{x}}$ and we get the signal $b = \boldsymbol{j}' \cdot \hat{\boldsymbol{x}}$. The numerical statistics are as following: $\langle b \rangle = 2a/3$ and $\sigma(b) = 1/\sqrt{3N}$. So, to get a $n\sigma$ detection,

$$N = 3n^2/4a^2 \tag{A1}$$

halos will be needed.

[1] Q. R. Ahmad *et al.*, Phys. Rev. Lett.**89**, 011301 (2002).
[2] K. A. Olive and Particle Data Group, Chinese Physics C **38**, 090001 (2014).
[3] P. A. R. Ade *et al.*, A&A**594**, A13 (2016).
[4] R. Laureijs *et al.*, ArXiv e-prints (2011), 1110.3193.
[5] LSST Science Collaboration *et al.*, ArXiv e-prints (2009), 0912.0201.
[6] K. S. Dawson *et al.*, Astron. J. **151**, 44 (2016).
[7] R. Goullioud *et al.*, Wide Field Infrared Survey Telescope [WFIRST]: telescope design and simulated performance, in *Space Telescopes and Instrumentation 2012: Optical, Infrared, and Millimeter Wave*, volume 8442 of Proc. SPIE, p. 84421U, 2012.
[8] D. Eisenstein and DESI Collaboration, The Dark Energy Spectroscopic Instrument (DESI): Science from the DESI Survey, in *American Astronomical Society Meeting Abstracts*, volume 225 of *American Astronomical Society Meeting Abstracts*, p. 336.05, 2015.
[9] H.-M. Zhu, U.-L. Pen, X. Chen, D. Inman, and Y. Yu, Phys. Rev. Lett.**113**, 131301 (2014), 1311.3422.
[10] H.-M. Zhu, U.-L. Pen, X. Chen, and D. Inman, Phys. Rev. Lett.**116**, 141301 (2016), 1412.1660.
[11] H.-R. Yu *et al.*, Nature Astronomy **1**, 0143 (2017).
[12] S. Codis *et al.*, MNRAS(2018), 1809.06212.
[13] S. D. M. White, ApJ**286**, 38 (1984).
[14] J. Lee and U.-L. Pen, ApJ**532**, L5 (2000), astro-ph/9911328.
[15] J. Lee and U.-L. Pen, ApJ**555**, 106 (2001), astro-ph/0008135.
[16] H.-R. Yu, U.-L. Pen, and X. Wang, The Astrophysical Journal Supplement Series **237**, 24 (2018).
[17] H.-M. Zhu, Y. Yu, U.-L. Pen, X. Chen, and H.-R. Yu, Phys. Rev. D**96**, 123502 (2017).
[18] Y. Yu, H.-M. Zhu, and U.-L. Pen, ApJ**847**, 110 (2017).
[19] H. Wang, H. J. Mo, X. Yang, Y. P. Jing, and W. P. Lin, ApJ**794**, 94 (2014), 1407.3451.
[20] H.-R. Yu, U.-L. Pen, and H.-M. Zhu, Phys. Rev. D**95**, 043501 (2017), 1610.07112.
[21] J. B. Peterson, K. Bandura, and U. L. Pen, ArXiv e-prints , astro (2006), astro-ph/0606104.
[22] G. Dvali and L. Funcke, Phys. Rev. D**93**, 113002 (2016).